

Quantification of Non Small Lung Lesions in PET/CT Imaging - A Feasibility Study using Monte Carlo Simulator Incorporating Digital Anthropomorphic Phantoms

B. Bouzid^{a*}, Y. Bouchareb^{b,c}, H. Gouraya^a and A. Cherfi^a

^a Laboratoire SNIRM, Faculté de Physique, USTHB, BP32, 16111, El Alia, Bab Ezzouar, Algeria.

^b Clinical Physics, Diagnostic & Therapeutic Division, Barts Health NHS Trust, London, UK.

^c Barts Cancer Institute, Queen Mary's University, London, UK.

*Corresponding author: bbouzid@usthb.dz



INTRODUCTION

Respiratory motion is a major problem in clinical PET/CT imaging. Breathing during data acquisition produces average motion images with limited image quality and reduced quantitative accuracy, leading to reduced detectability of lesions and reduced quantification of activity concentration.

In general, the approach used to reduce such problems is respiratory-gated acquisition of emission data based on the use of external sensors to measure the phase and / or amplitude of the respiratory cycle for sorting data acquired according to these information in separate respiratory bins. However, the use of such an approach in the clinic is difficult to implement and raises various problems¹. In this work, we used another approach based on Monte Carlo simulation while integrating an anthropomorphic phantom with lesions.

MATERIALS & METHODS

We have developed and validated a simulator of PET/CT Discovery-600[®] scanner (GE Healthcare, Fig. 1) using the GATE toolbox². The simulator was validated by comparing the Contrast Recovery Coefficients (CRCs) obtained using the IEC Image Quality phantom (Fig. 2, a and b) (as recommended by NEMA NU2-2007 standards) on the reconstructed images with the manufacturer's specifications and CRCs published in the literature.

For quantification purposes, a simulation of this scanner incorporating of the NCAT digital phantom⁷ was performed. Lung lesions simulated as spheres/ellipsoids of different sizes (10, 22 and 37 mm diameter) in different locations within the lungs' inserts of the NCAT phantom. Eight bins representing different phases in the respiratory cycle were simulated separately and summed to create realistic simulated images which incorporate respiratory motion effects.

All generated sinograms were reconstructed using the OSEM algorithm implemented in the STIR software library³. CRCs were calculated in the three lesions and compared with the CRCs obtained from the ones obtained on the IEC phantom. Simulations were performed on a computing cluster (112 core processors) over several months.

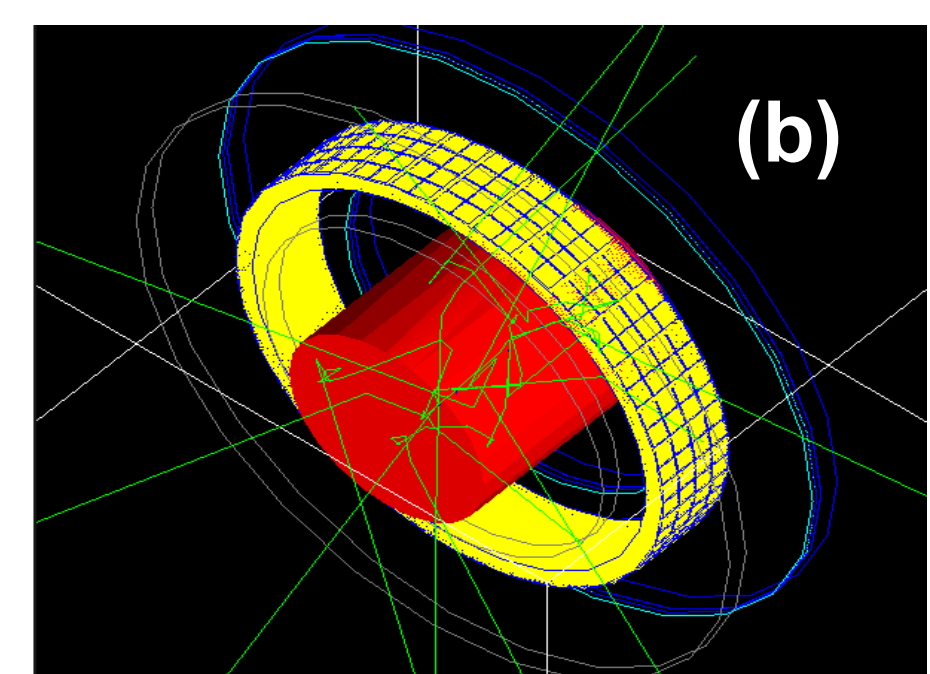


Fig. 1. (a) GE PET/CT Discovery-600 Camera (b) Simulation of PET D-600 camera and cylindrical phantom containing a linear source

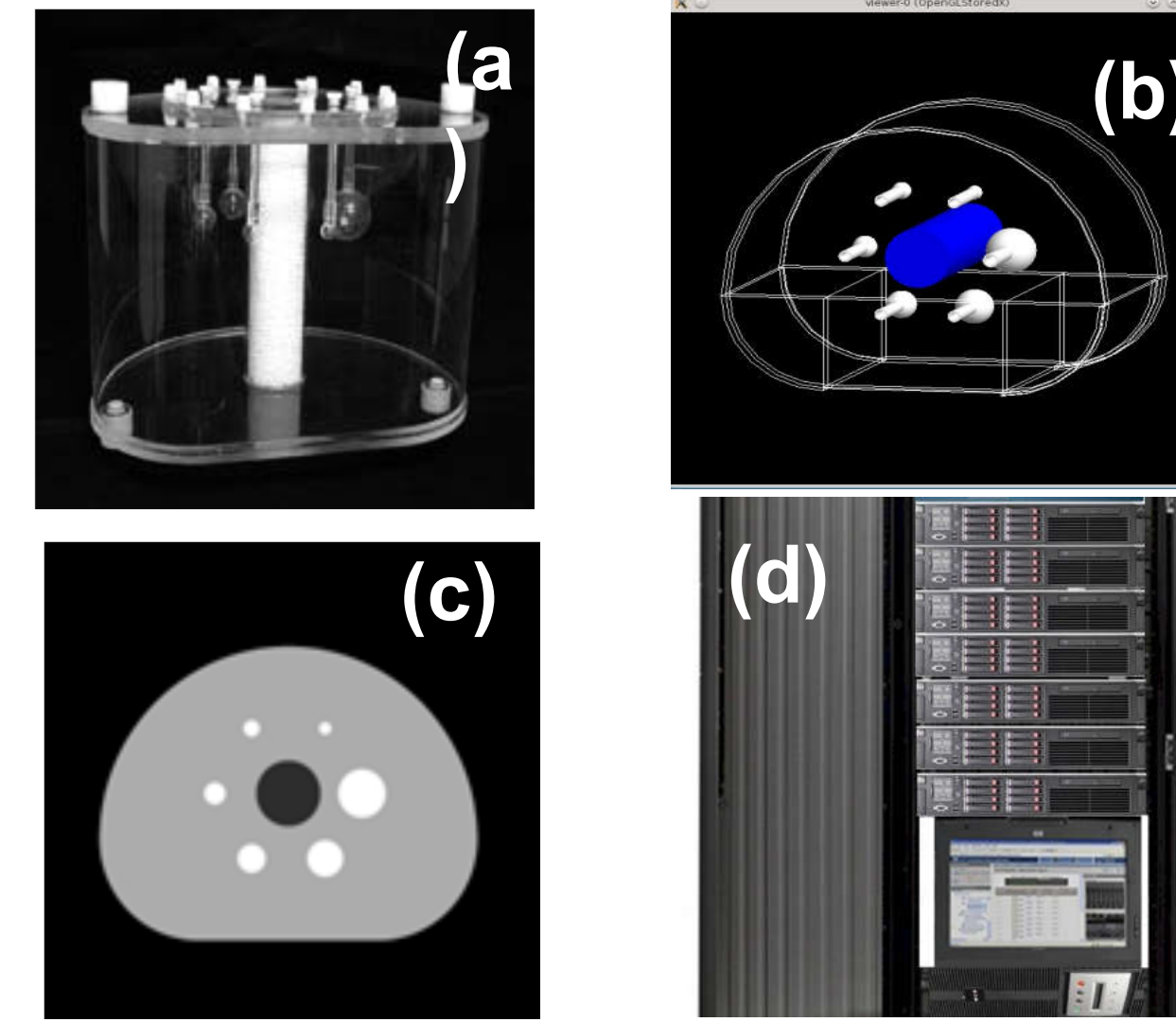


Fig. 2. (a) NEMA NU2-2007 phantom (b) NEMA 2007 body phantom modeled in GATE. The phantom is filled by 18F (5.3KBq / cm³). The four smallest spheres (diameters: 1.0, 1.3, 1.7, 2.2 cm.) are filled with 18F- water activity with a sphere to background activity ratio (SBR) of 4:1; The spheres (2.8 and 3.7 cm) are filled only with water. (c) μ -map image generated for the attenuation correction for Tomographic Image Reconstruction. (d) SNIRM laboratory cluster with 112 core

PURPOSE

The use of a PET/CT camera simulator incorporating digital anthropomorphic phantom is an effective tool to optimize and evaluate methods for correcting various spurious effects (attenuation, scatter, partial volume effect and respiratory movements). The aim of this study is to improve quantification of non-small lung lesions using a PET/CT camera simulator incorporating digital anthropomorphic phantom.

SIMULATOR VALIDATION

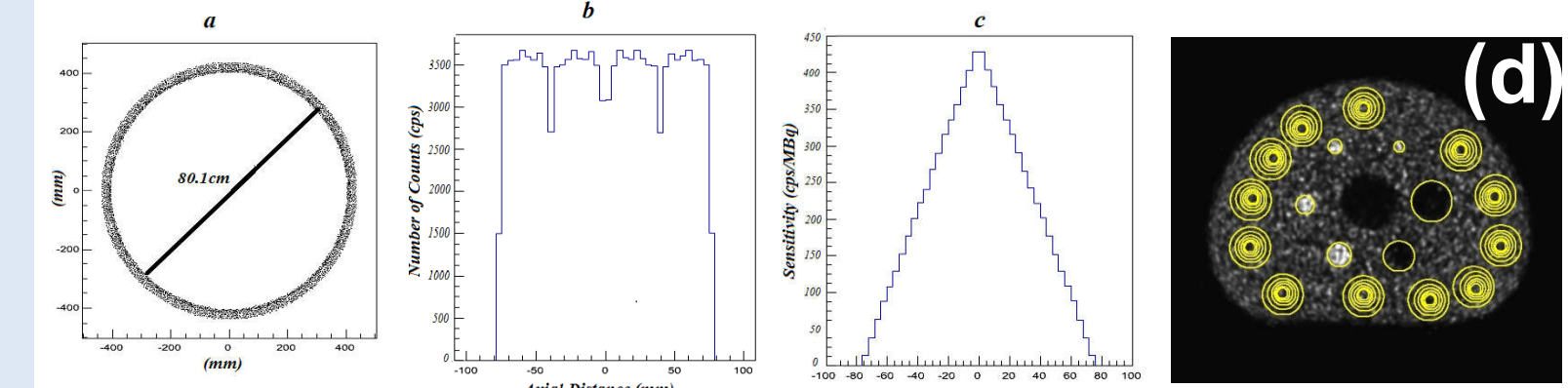


Fig. 3. (a) The D-600 transaxial detection position in x-y plan. (b) Axial detection position. (c) The 3D axial sensitivity. (d) Position of the regions of interest (ROIs) placed over the hot and cold spheres and the phantom background of the simulated and reconstructed images.

NEMA NU 2-2007 Tests	GE NEMA Test [4]	Measure s [5]	Simulation [6]	Simulation [Our work]	
Spatial Resolution	Transaxial @ 1cm	≤ 5.5	4.8	4.9	5.1
	Transaxial @ 10 cm	≤ 6.2	6.2	5.6	5.9
	Axial @ 1 cm	≤ 6.2	5.9	5.6	5.9
	Axial @ 10 cm	≤ 6.9	6.4	6.4	6.2
Sensitivity Average 0,10cm (cps/KBa)	≥ 8.2	9.6	9.22	8.97	
Scatter Fraction (%)	≤ 42	36.6	39.5	33.6	
NECR Count (Kcps)	≥ 68	75	89.7	80.1	
concentration (kBq/ml)	15	12.8	14.7	14.1	

Table 1. Simulator validation: Comparison of simulated spatial resolution, sensitivity, scatter fraction, noise equivalent count rate.

RESULTS

The hot sphere contrast recovery coefficient (HS_{CRC}), the cold sphere recovery coefficient (CS_{CRC}), the accuracy of attenuation and the scatter corrections in the lung region (DC_{lung}) and finally the background variability (BV) in percent (%) are given by the following relations:

$$HS_{CRC} = \left(\frac{(C_{hot}/C_{bkgd}) - 1}{(a_{hot}/a_{bkgd}) - 1} \right) \times 100; \quad CS_{CRC} = \left(1 - \left(\frac{C_{cold}/C_{bkgd}}{a_{cold}/a_{bkgd}} \right) \right) \times 100$$

$$DC_{lung} = \left(1 - \left(\frac{C_{lung}/C_{bkgd}}{SD/C_{bkgd}} \right) \right) \times 100; \quad BV = \left(\frac{SD/C_{bkgd}}{C_{bkgd}} \right) \times 100$$

where C_{hot} is the average measurement counts in the ROI for each hot sphere, C_{cold} is the count average measurement in the ROI for each cold sphere and C_{bkgd} is the average measurement count in the total of the 60 background ROIs of each size.

C_{lung} is the average measurement counts in ROI in the lung region that was drawn on each slice with 5 cm diameter.

SD is the standard deviation of the background ROI counts for each sphere.

a_{hot} and a_{bkgd} are the activity concentrations in the hot spheres and in the background respectively.

Sphere diameter (mm)	Hot sphere				Cold sphere	
	10	13	17	22	28	37
(HS_{CRC}) or (CS_{CRC}) (%) [4]	≥20	≥30	≥40	≥50	≥60	≥60
(HS_{CRC}) or (CS_{CRC}) (%) [Our measures]	43	50	60	61	75	82
BV (%) [4]	≤12	≤10	≤9	≤7	≤6	≤5
BV (%) [Our measures]	13	10	8	7	6	6
(DC_{lung}) [4]	≤19					
(DC_{lung}) [Our measures]	16					

Table 2: Image quality validation : Comparison between our simulation results and the manufacturer data⁴.

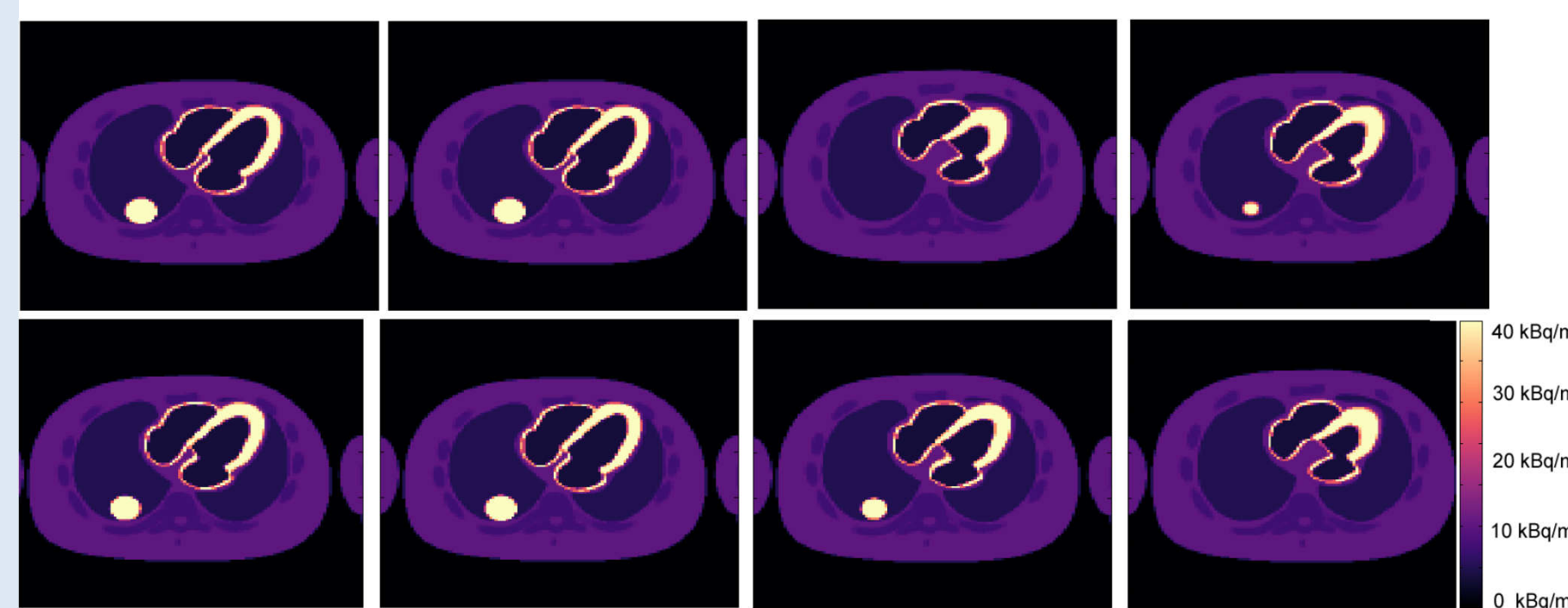


Fig. 3. NCAT digital phantom⁷ with simulated lung lesion as sphere (37mm diameter) with Eight bins representing different phases in the respiratory cycle.

The comparison of the CRCs obtained for all spheres by the simulation incorporating the IEC phantom with the manufacturer's specifications shows good correlation.

This demonstrates the efficiency of the developed simulator to reproduce the characteristics of the PET/CT Discovery-600 scanner. The CRCs calculated from the second simulation (NCAT phantom) for the 10, 22 and 37mm lesions are 35%, 24% and 15%, respectively lower compared to the first simulation (IEC phantom) due to respiratory induced artefacts in these lesions.

CONCLUSION

The finding of this study suggests that the parameterization used in the NCAT simulation provides more realistic CRCs which can be used on PET/CT clinical images to improve the quantification of non-small lung lesions.

REFERENCES

- [1] S. A. Nehmeh et al., "Effect of respiratory gating on quantifying PET images of lung cancer," J. Nucl. Med. 43, 876–881 (2002).2
- [2] S. Jan et al., GATE: a simulation toolkit for PET and SPECT. Phys Med Biol 49 (2004) 4543–4561. <http://www.opengatecollaboration.org>
- [3] K. Thielemans et al., " STIR: software for tomographic image reconstruction release 2 ". Phys Med Biol 57 (2012) 867–883. <http://stir.sourceforge.net>
- [4] GE Healthcare. DiscoveryTM PET/CT 600. NEMA Test Procedures. Direction 5401809-1EN, (2009)
- [5] E. De Ponti et al. Med. Phys. 38,(2011)968
- [6] H. Sheen et al., Journal of the Korean Physical Society, 65, No. 11, (2014)1802(L)
- [7] W.P. Segars et al. IEEE Nuclear Science Symposium Conference Record, vol.3, (2002) 1775